J. Fluid Mech. (1973), *vol.* 58, *part* 1, *pp.* 1–25
Printed in Great Britain

The origin of secondary flow in turbulent flow along a corner

By F. B. GESSNER
Department of Mechanical Engineering, University of Washington

(Received 13 March 1972 and in revised form 8 September 1972)

The mechanisms which initiate secondary flow in developing turbulent flow along a corner are examined on the basis of both energy and vorticity considerations. This is done by experimentally evaluating the terms of an energy balance and vorticity balance applied to the mean motion along a corner bisector. The results show that a transverse flow is initiated and directed towards the corner as a direct result of turbulent shear stress gradients normal to the bisector. The results further indicate that anisotropy of the turbulent normal stresses does not play a major role in the generation of secondary flow. Possible extensions of the present results to other related flow situations are illustrated and discussed.

1. Introduction

In developing turbulent flow along a corner, a transverse circulatory flow arises which is superimposed on the primary flow. This flow, which has been identified as secondary flow of the second kind by Prandtl (1952, p. 148), is of the same order of magnitude as the outward transverse flow associated with normal boundary-layer development, but differs from this flow because it is directed towards the wall in the vicinity of the corner bisector. As a consequence, secondary flow convects momentum, vorticity and energy of the mean motion into the corner and then, by virtue of continuity, these quantities are transported away from the corner along the bounding walls. A similar transport pattern applies for transferable quantities associated with the turbulent motion. This effect, in turn, distorts the local flow structure and, in particular, lines of constant axial mean velocity in planes normal to the axial flow direction (isotachs), as shown in figure 1. The distortion of isotach patterns in turbulent channel flow was perhaps first observed by Nikuradse (1926), who measured isotach distributions in channels of various cross-sectional shapes and found isotachs to be distorted in a manner indicative of secondary flow. Subsequent flow visualization studies by Nikuradse (1930) confirmed the existence of secondary flow in the form of streamwise helical vortices in the corner region.

The first explanation of this phenomenon was offered by Prandtl (1926), who suggested that secondary flow is caused by turbulent velocity fluctuations in regions of isotach curvature. In particular, Prandtl postulated that velocity fluctuations tangential to an isotach in regions of isotach curvature cause a transverse mean flow to develop which is directed from the concave towards

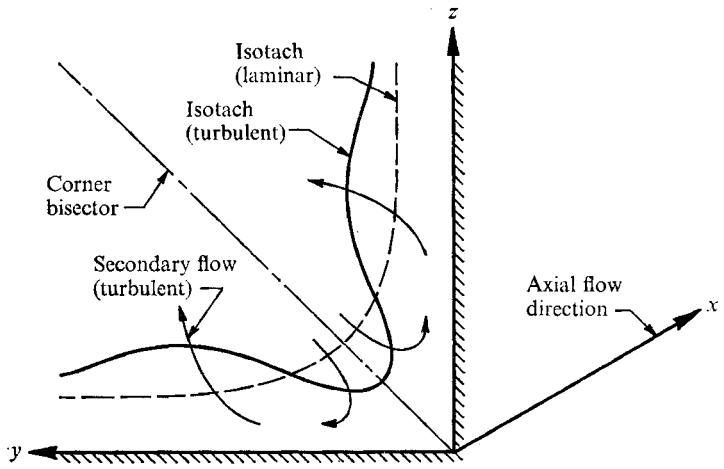

FIGURE 1. Typical isotach patterns for flow along a corner.

the convex side of the isotach, as shown in figure 1. Implicit in this model is the assumption that tangential velocity fluctuations at a given point on a curved isotach are greater than normal velocity fluctuations, a condition which has been verified experimentally by Gessner & Jones (1961).

Alternative explanations of the phenomenon have been proposed by Townsend (1961) and by Eichelbrenner and his co-workers (Eichelbrenner & Toan 1969; Eichelbrenner & Preston 1971); these are based on arguments related to the behaviour of certain terms in the transverse Reynolds equations. Other investigators suggest, however, that secondary flow arises because of streamwise vorticity which is generated in the corner region (Einstein & Li 1958; Brundrett & Baines 1964; Perkins 1970). The foregoing hypotheses are all based on arguments which presume cause-and-effect behaviour of certain flow variables in the corner region. In particular, all of these hypotheses assume, either explicitly or implicitly, that anisotropy of the transverse normal Reynolds stresses is responsible for the generation of secondary flow. In the discussion which follows, it will be shown that the normal Reynolds stresses do not have a dominant role in the generation of secondary flow, but that, instead, this flow is due primarily to Reynolds shear stress gradients in the corner region.

2. Development of the model

In order to write the governing system of equations in a form amenable to analysis, it is expedient to apply the boundary-layer approximations (cf. Hinze 1959, §7–2) to the equations of motion which describe steady, incompressible, developing turbulent flow along a corner. If the Reynolds stress components are all assumed to be of the same order of magnitude, then the Reynolds equations which apply outside the viscous sublayer can be written as

$$U\frac{\partial U}{\partial x}+V\frac{\partial U}{\partial y}+W\frac{\partial U}{\partial z}=-\frac{1}{\rho}\frac{\partial p}{\partial x}+\nu\left(\frac{\partial^2 U}{\partial y^2}+\frac{\partial^2 U}{\partial z^2}\right)-\frac{\partial \overline{uv}}{\partial y}-\frac{\partial \overline{uw}}{\partial z}, \tag{1}$$

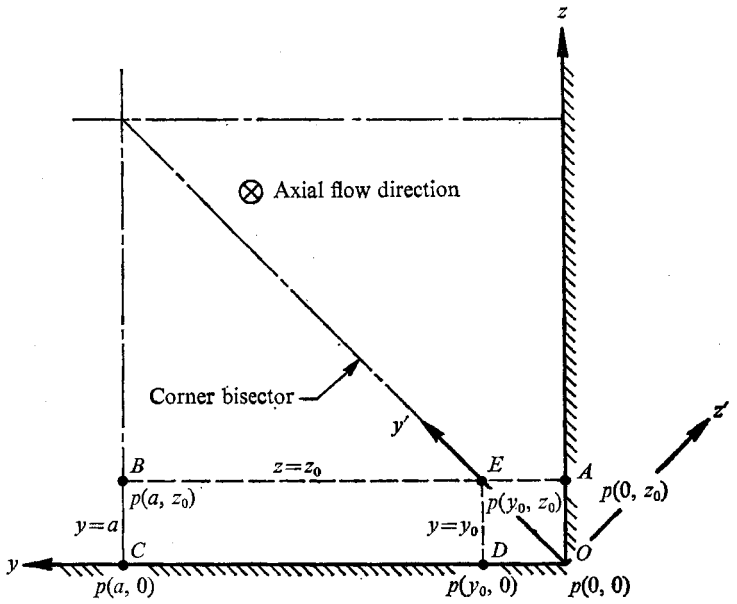

FIGURE 2. Static pressures at end-points of selected paths of integration.

$$\frac{1}{\rho}\frac{\partial p}{\partial y} = -\frac{\partial \overline{v^2}}{\partial y} - \frac{\partial \overline{vw}}{\partial z}, \tag{2}$$

$$\frac{1}{\rho}\frac{\partial p}{\partial z} = -\frac{\partial \overline{vw}}{\partial y} - \frac{\partial \overline{w^2}}{\partial z}, \tag{3}$$

where ρ is the fluid density, ν is the kinematic viscosity, p is the mean static pressure, U, V and W are mean velocity components, u, v and w are fluctuating velocity components in the x, y and z directions, respectively, and an overbar denotes a time-averaged quantity.

The above system of equations contains terms involving gradients of all Reynolds stress components except $\overline{u^2}$. It is thus difficult to determine from these equations whether turbulent shear or normal stress gradients are primarily responsible for the generation of secondary flow. An attempt has been made by Townsend (1961) to deduce the existence of secondary flow by integrating reduced forms of (2) and (3) along selected paths of integration normal to the bounding walls of a corner. In order to demonstrate this procedure, consider developing turbulent flow within a quadrant of a channel whose cross-section is square and whose sides are of length $2a$ (figure 2). If the transverse Reynolds equations are to be integrated along paths such as AB and BC shown in the figure (the procedure followed by Townsend), it is necessary to consider extended, rather than reduced, forms of (2) and (3), namely

$$\frac{\partial p}{\partial y} = -\rho\frac{\partial \overline{v^2}}{\partial y} - \rho\frac{\partial \overline{vw}}{\partial z} + \mu\left(\frac{\partial^2 V}{\partial y^2} + \frac{\partial^2 V}{\partial z^2}\right), \tag{4}$$

$$\frac{\partial p}{\partial z} = -\rho\frac{\partial \overline{vw}}{\partial y} - \rho\frac{\partial \overline{w^2}}{\partial z} + \mu\left(\frac{\partial^2 W}{\partial y^2} + \frac{\partial^2 W}{\partial z^2}\right), \tag{5}$$

since these paths originate at a bounding wall, extend through the viscous sublayer and terminate in the outer portion of the boundary layer. If (4) and (5) are integrated along the paths AB and BC respectively, then noting that

$$p(0, z_0) = p(y_0, 0)$$

on the basis of symmetry considerations, the pressure difference $p(a, 0) - p(y_0, 0)$ can be expressed as

$$p(a,0)-p(y_0,0) = \rho\overline{w^2}(a,z_0) - \rho\overline{v^2}(a,z_0) + \rho\int_0^{z_0}\left(\frac{\partial\overline{vw}}{\partial y}\right)_{y=a} dz - \rho\int_0^{a}\left(\frac{\partial\overline{vw}}{\partial z}\right)_{z=z_0} dy$$
$$+\mu\int_0^{a}\left(\frac{\partial^2 V}{\partial z^2}\right)_{z=z_0} dy - \mu\int_0^{z_0}\left(\frac{\partial^2 W}{\partial y^2}\right)_{y=a} dz - \mu\left(\frac{\partial V}{\partial y}\right)_{0,z_0} + \mu\left(\frac{\partial W}{\partial z}\right)_{a,0}, \qquad (6)$$

in which the viscous terms $\mu\partial V/\partial y$ and $\mu\partial W/\partial z$ evaluated at (a, z_0) have been omitted, but all other terms which are not identically zero have been retained. An alternative expression can be developed for his pressure difference by integrating (4) along the path CD to yield

$$p(a,0)-p(y_0,0) = -\rho\int_{y_0}^{a}\left(\frac{\partial\overline{vw}}{\partial z}\right)_{z=0} dy + \mu\int_{y_0}^{a}\left(\frac{\partial^2 V}{\partial z^2}\right)_{z=0} dy, \qquad (7)$$

in which the terms $\mu\partial V/\partial y$ evaluated at $(a, 0)$ and $(y_0, 0)$ have been deleted because $V = 0$ along the wall $z = 0$.

Equations (6) and (7) are alternative expressions for the pressure difference $p(a, 0) - (y_0, 0)$ and are mutually compatible equations. In the development given by Townsend, however, the viscous and turbulent shear stress terms in (4) and (5) are omitted, in turn, resulting in an apparent pressure anomaly along the wall $z = 0$. This anomalous behaviour occurs because the reduced form of (7) which applies when the shear stress terms are deleted predicts that $p(a, 0) - p(y_0, 0)$ is zero, whereas the corresponding reduced form of (6) predicts that this pressure difference is equal to $\rho\overline{w^2}(a, z_0) - \rho\overline{v^2}(a, z_0)$, which is not equal to zero because $\overline{w^2}(a, z_0) < \overline{v^2}(a, z_0)$ within the interval $0 < z_0 < a$ (cf. Brundrett & Baines 1964, figure 7). In order to eliminate this apparent anomaly, Townsend suggests that a transverse circulatory flow pattern must be present in which the fluid motion is directed from the corner towards the wall bisector near a bounding wall. On the basis of (6) and (7), however, it is evident that no pressure anomaly actually exists, and consequently arguments based on anomalous pressure behaviour cannot be used to explain the origin of secondary flow.

An alternative model for the generation of secondary flow has been suggested by Eichelbrenner & Preston (1971), and is based on wall static pressure behaviour in the corner region coupled with the asymptotic behaviour of the transverse normal Reynolds stresses at the outer edge of the boundary layer. In formulating the model, (2) is first rewritten in terms of y', z' co-ordinates shown in figure 2 and then integrated along the path OE to yield an expression for $p(y, z_0)$ at the point E, which is stipulated as being at the outer edge of the boundary layer. An alternative expression for $p(y_0, z_0)$ is also developed by integrating (3) along the path DE and assuming that $\partial\overline{vw}/\partial y \simeq 0$ along this path. The resulting expressions are then compared, and it is shown that $p(0, 0) > p(y_0, 0)$ or, equivalently, that a transverse static pressure gradient exists along the wall $z = 0$ in the near

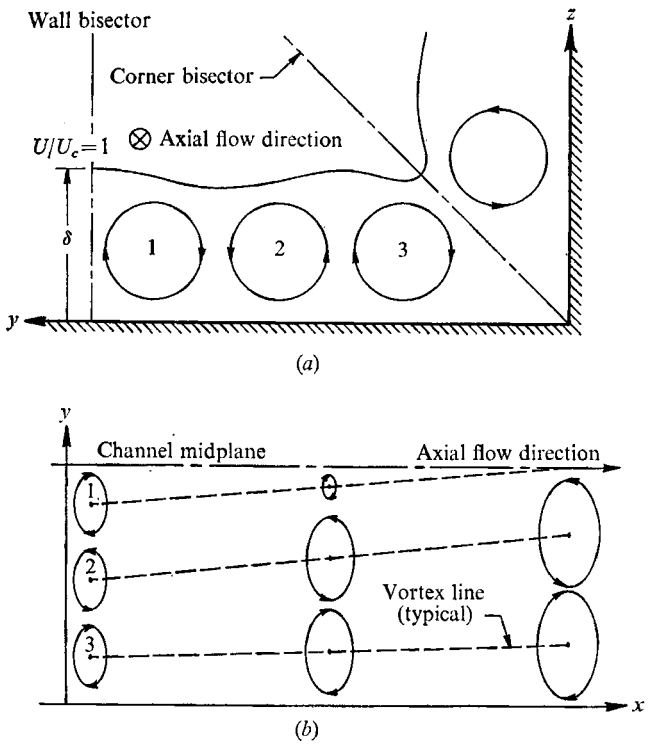

FIGURE 3. Model of secondary flow development proposed by Eichelbrenner & Preston (1971). (*a*) Multi-vortex flow structure in corner region. (*b*) Displacement of vortex lines in the axial flow direction (view on plane $z = 0$).

vicinity of the corner. On the basis of this result, the authors state that a secondary-flow vortex will be created within the triangle *OED* and, in fact, that a multi-vortex flow structure will be induced adjacent to the bounding walls of a corner as long as the flow is still developing (figure 3*a*). The authors then reason that, for flow in a square channel, vortex lines of the secondary flow vortices will converge toward the channel midplane as the flow develops (figure 3*b*), with the vortices closest to the midplane eventually collapsing until only one secondary-flow vortex exists in each octant of the channel cross-section. Implicit in the above reasoning is: (i) the existence of a series of static pressure maxima and minima along the bounding walls of a corner for developing flow; (ii) an undulating isotach pattern, as indicated by the isotach $U/U_c = 1$ in figure 3(*a*); and (iii) both positive and negative values of W in the boundary layer above the wall $z = 0$.

In order to investigate whether or not this behaviour actually occurs, measurements of wall static pressure, primary-flow velocity and secondary-flow velocity were made in the present study in the developing flow region of a square channel. The details of the apparatus and the experimental techniques that were used are discussed in the appendix. For the present, it will suffice to note that no undulations in the isotach pattern were observed at $x/D_h = 4,8$, where x is the axial distance measured from the channel inlet and D_h is the hydraulic diameter of the channel (figure 4). Furthermore, at $x/D_h = 8$, measurements of W at intervals of

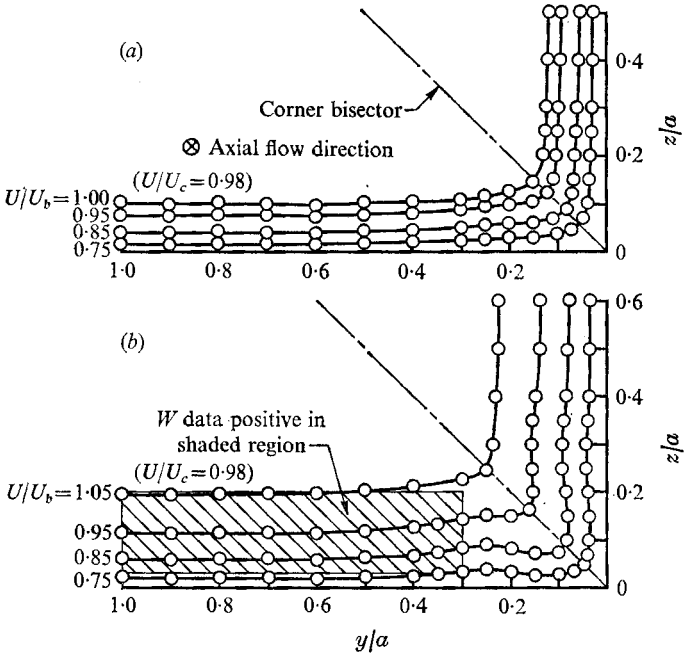

FIGURE 4. Isotach distributions in developing flow region of square channel; $Re_b = 2{\cdot}5 \times 10^5$. (a) $x/D_h = 4$. (b) $x/D_h = 8$.

$\Delta y/a = 0{\cdot}1$ within the range $0{\cdot}3 \leqslant y/a \leqslant 1{\cdot}0$ indicated that W was positive (directed away from the wall $z = 0$) at all measuring points. Wall static pressure measurements at $x/D_h = 4,8$ within the interval $0{\cdot}01 \leqslant y/a \leqslant 1$ also showed no discernible variations to within the resolution accuracy of the micromanometers used for this particular measurement ($\pm 0{\cdot}001$ in. water).† At $Re_b \equiv U_b D_h/\nu = 2{\cdot}5 \times 10^5$, for example, the normalized incremental wall static pressure difference $\Delta p/(\frac{1}{2}U_c^2)$ was less than $\pm 0{\cdot}0015$, where U_b and U_c are the bulk and core flow velocities in the axial flow direction, respectively. It would appear, therefore, that the multivortex flow structure proposed by Eichelbrenner & Preston is non-existent, at least for developing turbulent flow in a square channel, and consequently the model they propose cannot be applicable to all turbulent corner flows.

The foregoing discussion centred on proposed models for the generation of secondary flow which are based on the behaviour of certain terms in the transverse Reynolds equations. A modified form of these equations has been considered by Gessner & Jones (1965), who developed a momentum balance in terms of streamline co-ordinates referred to the secondary flow. In that study each term in an equation applicable to flow along a particular secondary-flow streamline was evaluated experimentally, with the exception of the static pressure term, which was used as a closing entry. On the basis of this information, the authors concluded that secondary flow originates because of small differences

† It should be noted that these results do not imply that the wall static pressure was identically constant along the wall $z = 0$ because variations in wall static pressure do exist along the bounding walls of a corner of the basis of (6) and (7). These variations were not detected in the present study because of resolution limitations of the instrumentation.

between transverse static pressure and Reynolds stress gradients in the flow. Their conclusions are not definitive, however, because the term indicative of momentum transport by the secondary flow was two orders of magnitude less than the static pressure and Reynolds stress terms in the equation.

In addition to the hypotheses discussed above, other hypotheses have been proposed which are based on the behaviour of certain terms in the axial vorticity equation. In turbulent corner flow studies the origin of secondary flow has been attributed primarily to the formation of streamwise vorticity in the flow (Brundrett & Baines 1964; Perkins 1970), whereas secondary flow in bounded rectangular jets is thought to originate because vortex filaments normal to the axial flow direction are stretched and reoriented near the bounding walls of the jet (Foss & Jones 1968). Both of the mechanisms cited above result in the development of axial vorticity in the flow. In turbulent corner flow, for example, it is possible to deduce that ξ, the axial vorticity component of the mean motion, will be zero on a corner bisector and of opposite sign on either side of the bisector, as shown in figure 5(*a*). This behaviour is consistent with the resultant secondary-flow patterns shown in figure 5(*b*) if it is noted that ξ and $\mathbf{U}_s$ are interrelated as follows:

$$\Gamma = \int_A \xi dA = \oint_C \mathbf{U}_s . d\mathbf{r}, \tag{8}$$

in which Γ is the circulation, $d\mathbf{r}$ is a differential position vector along C, a simple closed curve in the y, z plane, and A is the area bounded by that curve. A positive value of ξ thus is indicative of clockwise vorticity, which, on the basis of (8), is consistent with the clockwise secondary-flow patterns shown in figure 5(*b*). It should not be inferred from this behaviour, however, that the mechanisms which cause streamwise vorticity to develop in turbulent flow along a corner (figure 5*a*) are necessarily responsible for the initiation of secondary flow, i.e. the transverse circulatory-flow patterns shown in figure 5(*b*).

In order to determine the mechanism(s) responsible for the generation of secondary flow from a vorticity point of view, it is expedient to examine the vorticity transport equations for the mean motion after the boundary-layer approximations have been applied. If it is again assumed that all Reynolds stress components are of the same order of magnitude, and if η and ζ are defined as the mean vorticity components in the y and z directions, respectively, the resulting vorticity equations can be written as

$$0 = \frac{\partial^2 \overline{v^2}}{\partial y \partial z} - \frac{\partial^2 \overline{w^2}}{\partial y \partial z} + \frac{\partial^2 \overline{vw}}{\partial z^2} - \frac{\partial^2 \overline{vw}}{\partial y^2}, \tag{9}$$

$$U\frac{\partial \eta}{\partial x} + V\frac{\partial \eta}{\partial y} + W\frac{\partial \eta}{\partial z} = \nu\left(\frac{\partial^2 \eta}{\partial y^2} + \frac{\partial^2 \eta}{\partial z^2}\right) + \eta\frac{\partial V}{\partial y} + \zeta\frac{\partial V}{\partial z} - \frac{\partial^2 \overline{uv}}{\partial y \partial z} - \frac{\partial^2 \overline{uw}}{\partial z^2}, \tag{10}$$

$$U\frac{\partial \zeta}{\partial x} + V\frac{\partial \zeta}{\partial y} + W\frac{\partial \zeta}{\partial z} = \nu\left(\frac{\partial^2 \zeta}{\partial y^2} + \frac{\partial^2 \zeta}{\partial z^2}\right) + \eta\frac{\partial W}{\partial y} + \zeta\frac{\partial W}{\partial z} + \frac{\partial^2 \overline{uw}}{\partial y \partial z} + \frac{\partial^2 \overline{uv}}{\partial y^2}, \tag{11}$$

in which $\eta \simeq \partial U/\partial z$, $\zeta \simeq -\partial U/\partial y$, and all terms are of the same order of magnitude, at least on the basis of the applied boundary-layer approximations.

If the order of magnitude of terms in equations (9)–(11) is designated as

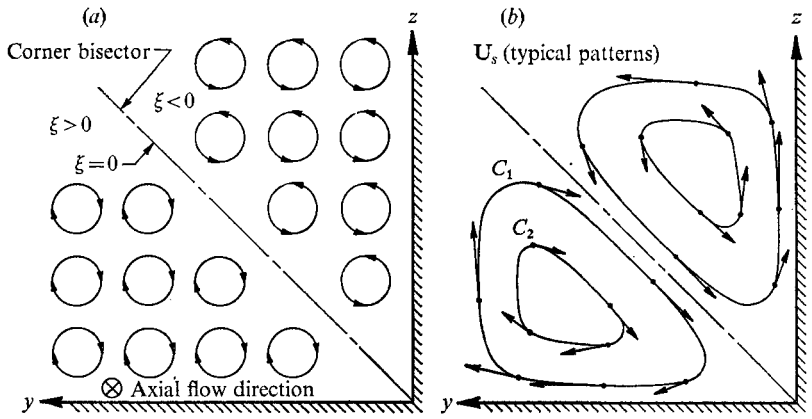

FIGURE 5. Experimentally observed (*a*) axial vorticity behaviour and (*b*) secondary-flow velocity patterns in the corner region.

unity, then the next higher order terms which have been omitted in equation (9) are of the order L_2/L_1, where L_1 and L_2 are characteristic boundary-layer length scales in the axial and transverse flow directions, respectively, and $L_2 \ll L_1$. The measurements of Perkins (1970) indicate, however, that the terms on the right-hand side of equation (9), when grouped together in the form of differences, are only of the same order of magnitude as the next higher order terms omitted in (9). On the basis of these considerations, a modified form of (9) actually applies for the ξ component of mean vorticity, namely

$$U\frac{\partial\xi}{\partial x}+V\frac{\partial\xi}{\partial y}+W\frac{\partial\xi}{\partial z}=\nu\left(\frac{\partial^2\xi}{\partial y^2}+\frac{\partial^2\xi}{\partial z^2}\right)+\xi\frac{\partial U}{\partial x}+\eta\frac{\partial V}{\partial y}+\zeta\frac{\partial U}{\partial z}$$
$$+\frac{\partial}{\partial x}\left(\frac{\partial\overline{uv}}{\partial z}-\frac{\partial\overline{uw}}{\partial y}\right)+\frac{\partial^2}{\partial y\,\partial z}(\overline{v^2}-\overline{w^2})+\left(\frac{\partial^2}{\partial z^2}-\frac{\partial^2}{\partial y^2}\right)\overline{vw}, \quad (12)$$

in which $\xi = \partial W/\partial y - \partial V/\partial z$, $\eta = \partial U/\partial z - \partial W/\partial x$, $\zeta = \partial V/\partial x - \partial U/\partial y$, and all terms are at least an order of magnitude less than the terms in (10) and (11). The foregoing results indicate that (12) describes only a second-order effect and that (10) and (11) are the equations which should be considered in examining the reasons why secondary flow develops from a vorticity point of view. These equations contain terms on the left-hand side which represent the convective transport of primary-flow vorticity by the secondary flow. The mechanism by which this transport process originates can be demonstrated most readily by experimentally evaluating the terms in (11) after this equation has been written along a corner bisector in terms of the x, y' and z' co-ordinates shown in figure 2, and, indeed, this course of action will be pursued later in the paper. For the present, however, discussion will centre on energy concepts applied to the flow in order to develop a model which is more amenable to interpretation from a conceptual point of view.

The only previous study in which energy concepts have been applied to turbulent corner flow is that of Hinze (1967), who examined the behaviour of terms in a mechanical energy balance applied to the turbulent motion. More specifically, Hinze showed that a transverse mean flow must be present whenever the produc-

tion of turbulent energy differs from the dissipation at a particular point in the flow. This transverse flow is in the form of a convective transport of turbulence kinetic energy by the secondary flow, and the production and dissipation terms responsible for this transport process include both shear stress components of the Reynolds stress tensor and correlations between components of the instantaneous turbulent rate of strain tensor.

On the basis of the above comments it would appear that both turbulent stresses and strain rates must be considered in examining the conditions under which secondary flow will occur. It is not necessary to follow this approach, however, because the mechanism by which secondary flow originates is clearly discernible if one examines an energy balance applied to the mean motion. This can be done most conveniently by considering an energy balance along a corner bisector written in terms of the x, y' and z' co-ordinates shown in figure 2. The reduced form of the equation that applies after the boundary-layer approximations have been introduced is the following:

$$\underset{I\,A}{\frac{U}{\rho}\frac{\partial P_0}{\partial x}} + \underset{I\,B}{\frac{V'}{\rho}\frac{\partial P_0}{\partial y'}} - \nu\left[\underset{II\,A}{\frac{\partial}{\partial y'}\left(U\frac{\partial U}{\partial y'}\right)} + \underset{II\,B}{\frac{\partial}{\partial z'}\left(U\frac{\partial U}{\partial z'}\right)}\right] + \underset{II\,C}{\frac{\partial}{\partial y'}(U\overline{uv'})} + \underset{II\,D}{\frac{\partial}{\partial z'}(U\overline{uw'})} - \underset{III}{\overline{uv'}\frac{\partial U}{\partial y'}} + \underset{IV}{\nu\left(\frac{\partial U}{\partial y'}\right)^2} = 0, \quad (13)$$

where V' is the secondary-flow velocity component in the y' direction,

$$P_0 \equiv p + \tfrac{1}{2}\rho(U^2 + V'^2 + W'^2)$$

is the total pressure of the mean flow and $\overline{uv'}$ and $\overline{uw'}$ are Reynolds shear stress components acting in the x, y' and x, z' planes, respectively.

In (13) each term can be interpreted as either a loss or gain in mean flow energy within an inertial volume element on the corner bisector depending, respectively, on whether the term is a positive or negative quantity. The sign of some of the terms can be determined by examining the experimental results of previous corner flow studies by Perkins (1970) and Gessner (1964), which apply for developing turbulent flow along a corner and fully developed turbulent corner flow, respectively. From the data of these two studies it is possible to deduce, for example, that terms $I\,A$ and $I\,B$ in (13) are both negative. More specifically, these terms are negative because the data show that $U > 0$ and $\partial P_0/\partial y' > 0$ along a corner bisector for flow under favourable pressure gradients, whereas $V' < 0$ in the boundary layer (i.e. V' is directed toward the corner) and, of course, $\partial P_0/\partial x < 0$ because of viscous effects in the flow.

The negative sign of both $I\,A$ and $I\,B$, in turn, implies a net flux of energy into a volume element on the corner bisector or, equivalently, a gain in mean flow energy within that element. The mechanism by which this gain in energy occurs can be interpreted as a net convective transport of mean flow energy into the volume element by the primary ($I\,A$) and secondary flows ($I\,B$), respectively. This behaviour implies that energy losses must occur within the volume element which necessarily lead to a transverse convective transport of mean flow

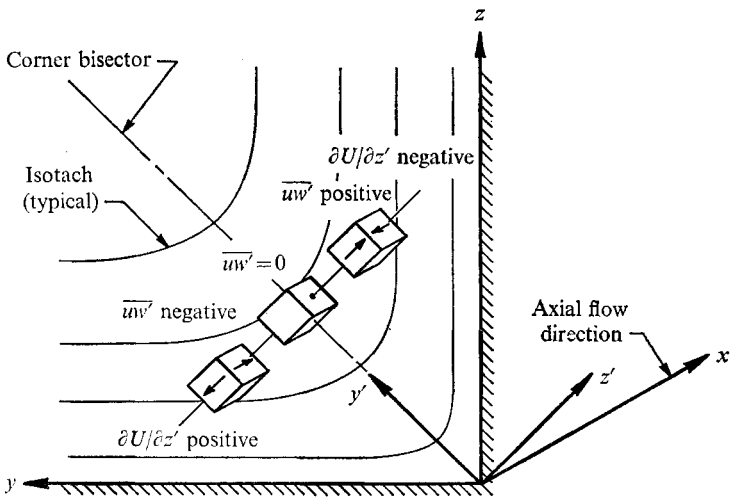

FIGURE 6. Origin of transverse turbulent shear stress gradients in transitional corner flow.

energy by the secondary flow. The problem, therefore, is to decide which of the energy transfer processes associated with the remaining terms in (13) is primarily responsible for the initiation of this transport process.

The remaining terms in (13) represent the work done by the mean flow against gradients of the viscous (IIA and IIB) and turbulent (IIC and IID) shear stresses, the production of turbulent energy from the mean flow (III), and the viscous dissipation of mean flow energy (IV). On the basis of data obtained by Brundrett (1963) and Gessner (1964) for fully developed flow, it is reasonable to presume that IIA, IIB, III and IV are negative in sign for developing turbulent flow along a corner or, equivalently, that each term corresponds to a loss in mean flow energy at points along a corner bisector. Term IIC may or may not correspond to a loss depending on the relative rates at which U increases and $-\overline{uv'}$ decreases in the y' direction. The foregoing terms, with the exception of IIB and IID, are all indicative of loss mechanisms in fully developed, two-dimensional turbulent boundary-layer flow where secondary flow is non-existent. It is reasonable to presume, therefore, that gradients associated with these terms will have a minimal influence on the generation of secondary flow in three-dimensional turbulent corner flow. Furthermore, it is also reasonable to presume that the energy losses associated with IIB do not play a dominant role because viscous effects are generally confined to the immediate vicinity of a wall, and thus viscous stresses cannot initiate or maintain a transverse flow in the outer portion of the boundary layer. It would appear therefore that energy losses associated with the only remaining term in (13), namely IID, must be the loss mechanism primarily responsible for the initiation of secondary flow.

The validity of this argument can be examined by considering developing flow along a corner when the flow is in a state of transition. In this type of flow it is known that isotachs in the near-corner region are as shown in figure 6 when turbulent bursts first appear locally in the flow (Zamir & Young 1970). Under

these circumstances $\partial U/\partial z'$ is positive for $z' < 0$ and it is reasonable to presume that positive w' fluctuations in this region generally give rise to negative u fluctuations, so that $\overline{uw'}$ is negative. This type of reasoning is analogous to the reasoning that is used to deduce that $\overline{uv}$ is negative whenever $\partial U/\partial y$ is positive in two-dimensional turbulent boundary-layer flows with no velocity maxima or minima in the boundary layer. If the foregoing argument is valid, then the converse must also be true, namely that $\overline{uw'}$ is positive for $z' > 0$ since $\partial U/\partial z'$ is negative in this region.

On the basis of the preceding arguments it follows that $\partial\overline{uw'}/\partial z'$ is positive, in general, at points along a corner bisector for transitional corner flow. This behaviour implies that $\partial(U\overline{uw'})/\partial z'$ is also positive and, consequently, a mechanism exists by which energy losses will occur which could possibly exceed other losses in the flow. If the primary flow cannot convect sufficient energy into volume elements on the bisector to compensate for these losses, then a transverse flow must be initiated which transports a net influx of energy into these volume elements. This statement is equivalent to saying that the energy transfer mechanisms associated with terms $\mathrm{I}B$ and $\mathrm{II}D$ in (13) may well be dominant in transitional flow so that energy losses incurred by the working of the mean flow against transverse turbulent shear stress gradients necessarily give rise to a convective transport of mean flow energy into the corner region in order to maintain dynamic equilibrium.

The validity of this hypothesis can be examined by experimentally evaluating the terms of (13) for transitional flow along a corner. This procedure can lead to experimental difficulties, however, because large-scale transitional boundary layers are difficult to realize in practice and the flow is inherently unstable. As an alternative approach, it would be more expedient to evaluate the terms of (13) for fully developed turbulent corner flow if it can be shown that the principal mechanism which *maintains* the secondary flow in this case is equivalent to the mechanism which *initiates* this transverse flow when the overall flow is in a state of transition. This equivalency can be demonstrated if it is first noted that (13) still applies along a corner bisector with no reduction in the number of terms or alteration in the sign of each term when the flow is fully developed. Furthermore, the preceding arguments which were used to eliminate all energy losses except those associated with the term $\mathrm{II}D$ in (13) as the possible initiating loss mechanism are also applicable to fully developed flow. It follows, therefore, that, if the energy losses associated with $\mathrm{II}D$ are responsible for the generation of secondary flow, they must also be responsible for maintaining secondary flow in a corner region when the flow is fully developed.

3. Results and discussion

In order to examine the validity of the proposed model, turbulence and mean flow measurements were made in a 10×10 in. square channel at $x/D_h = 84$, where the flow was essentially fully developed. Corner region measurements were made either along or normal to the bisector $z' = 0$ for a bulk Reynolds number of $2{\cdot}5 \times 10^5$; details of the measuring techniques are given in the appendix. The

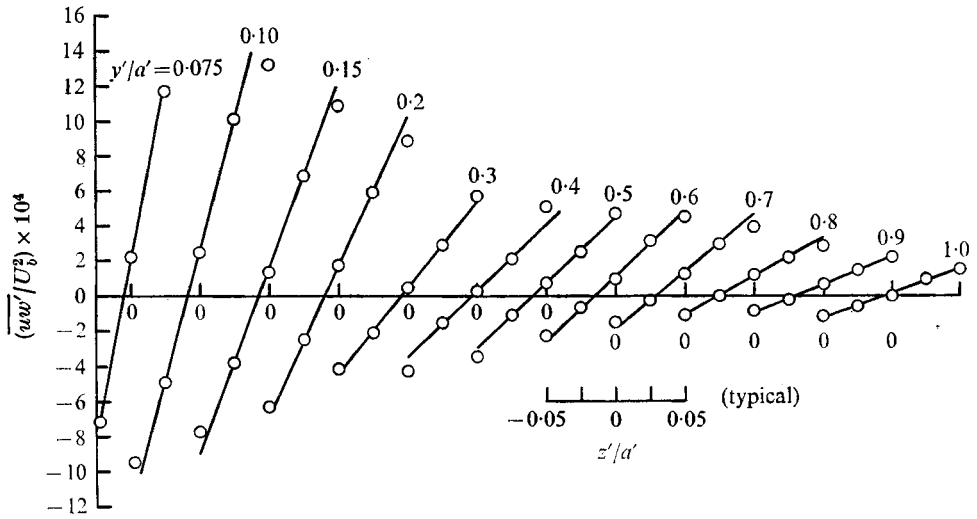

FIGURE 7. Turbulent shear stress distributions along normals to the corner bisector $z' = 0$; $Re_b = 2{\cdot}5 \times 10^5$.

non-dimensionalized $\overline{uw'}$ stress values measured along normals to the corner bisector are shown in figure 7. These measurements were made at transverse intervals of 0·177 in. ($\Delta z'/a = 0{\cdot}025$) along normals to the bisector between the corner and the axial centre-line of the channel ($y'/a' = 1{\cdot}0$). The stress values shown in figure 7 are generally negative for $z' < 0$ and positive for $z' > 0$ which is in accordance with anticipated behaviour based on earlier considerations.

The relative influence of the stress gradients shown in figure 7 on energy losses in the flow was examined by experimentally evaluating each term in a non-dimensionalized form of (13), namely

$$\underset{I\,A}{U^*\frac{\partial P_0^*}{\partial x^*}} + \underset{I\,B}{V'^*\frac{\partial P_0^*}{\partial y'^*}} - \frac{1}{Re_b}\left[\underset{II\,A}{\frac{\partial}{\partial y'^*}\left(U^*\frac{\partial U^*}{\partial y'^*}\right)} + \underset{II\,B}{\frac{\partial}{\partial z'^*}\left(U^*\frac{\partial U^*}{\partial z'^*}\right)}\right]$$

$$+ \underset{II\,C}{\frac{\partial}{\partial y'^*}(U^*\overline{uv'^*})} + \underset{II\,D}{\frac{\partial}{\partial z'^*}(U^*\overline{uw'^*})} - \underset{III}{\overline{uv'^*}\frac{\partial U^*}{\partial y'^*}} + \underset{IV}{\frac{1}{Re_b}\left(\frac{\partial U^*}{\partial y'^*}\right)^2} = 0, \quad (14)$$

in which

$$x^* \equiv x/D_h, \quad y'^* \equiv y'/D_h, \quad z'^* \equiv z'/D_h, \quad U^* \equiv U/U_b, \quad V'^* \equiv V'/U_b,$$
$$\overline{uv'^*} \equiv \overline{uv'}/U_b^2, \quad \overline{uw'^*} \equiv \overline{uw'}/U_b^2, \quad P_0^* \equiv P_0/(\rho U_b^2), \quad Re_b \equiv U_b D_h/\nu.$$

The results of this evaluation are shown in figure 8. The distributions indicate that the energy fluxes associated with IB and IID dominate the flow, except in the outer portion of the boundary layer. In the corner region, the energy losses incurred by the working of the mean flow against turbulent shear stress gradients along the bisector (IIC) and against gradients of the viscous stresses (IIA and IIB) are negligible in comparison with the losses which result from transverse shear stress gradients in the flow (IID). From the figure it is also evident that dissipation losses (IV) are negligible over most of the boundary layer, and that

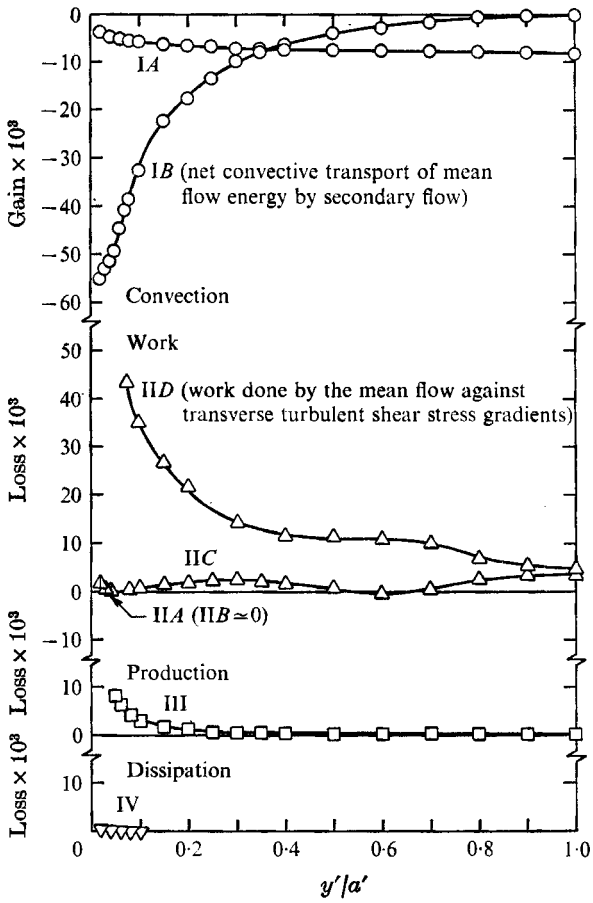

FIGURE 8. Distribution of terms in (14) along the corner bisector $z' = 0$; $Re_b = 2{\cdot}5 \times 10^5$.

the losses which result from the production of turbulent energy from the mean flow (III) are small in comparison with the losses associated with IID, even in the near-wall region. Within the interval $0 < y'/a' \lesssim 0{\cdot}7$ it is apparent that the primary flow cannot convect sufficient mean flow energy (IA) into volume elements on the bisector to compensate for the energy losses which occur within these elements. The only mechanism available to compensate for this difficiency is additional convective transport into these elements, and therefore a transverse flow which transports a net flux of energy into these elements (IB) must be present in order to maintain dynamic equilibrium. In the outer region of the boundary layer ($y'/a' \gtrsim 0{\cdot}8$), figure 8 indicates that IB, IIA, IIB, III and IV in (14) are negligible, and that energy losses which occur within a volume element by the working of the mean flow against turbulent shear stress gradients in the flow (IIC and IID) are essentially balanced by a net convective transport of mean flow energy into that volume element by the primary flow (IA). The above results are shown in alternative form in figure 9, where the sum of terms is indicative of the overall accuracy of the experimental measurements.

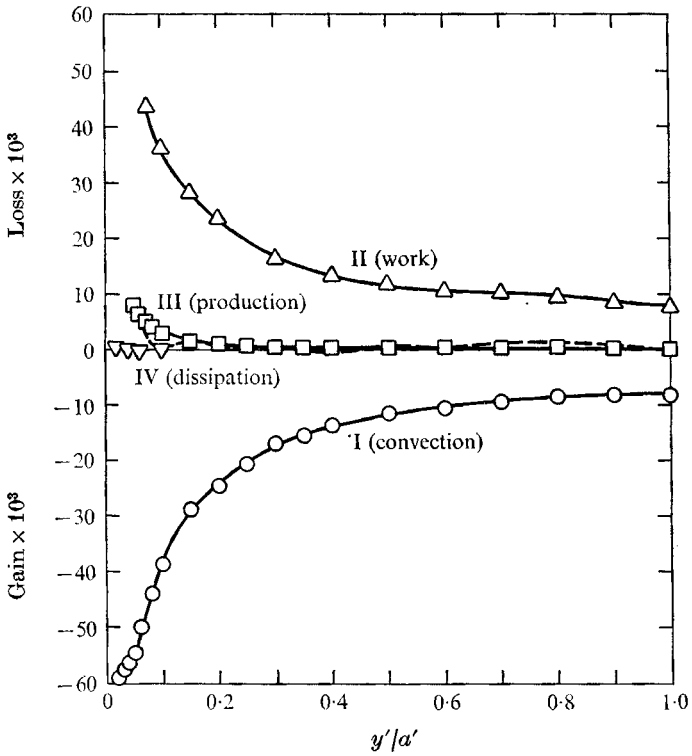

FIGURE 9. Energy balance for the mean motion along the corner bisector $z' = 0$; $Re_b = 2{\cdot}5 \times 10^5$. – – –, I+II+III+IV.

The preceding remarks apply qualitatively to transitional flow along a corner, where the working of the mean flow against transverse turbulent shear stress gradients in the corner region can now be regarded as the mechanism which both initiates and maintains the secondary flow. As noted earlier, the origin of secondary flow can also be explained from a vorticity point of view. Although transverse convective transport of mean flow vorticity and mean flow energy are actually different manifestations of the same phenomenon, an explanation of secondary flow based on vorticity considerations will be pursued in order to demonstrate that the origin of secondary flow can be fully explained by means of vorticity arguments without recourse to the axial vorticity equation. If (10) and (11) are written in terms of the x, y' and z' co-ordinates shown in figure 6, then all terms of (10) are identically zero along a corner bisector and the non-dimensionalized form of (11) which applies along the corner bisector $z' = 0$ for fully developed flow is the following:

$$\underset{\text{I}}{V'^*\frac{\partial \zeta'^*}{\partial y'^*}} - \underset{\text{II}A}{\frac{1}{Re_b}\frac{\partial^2 \zeta'^*}{\partial y'^{*2}}} - \underset{\text{II}B}{\frac{1}{Re_b}\frac{\partial^2 \zeta'^*}{\partial z'^{*2}}} - \underset{\text{III}A}{\frac{\partial^2 \overline{uv'}^*}{\partial y'^{*2}}} - \underset{\text{III}B}{\frac{\partial^2 \overline{uw'}^*}{\partial y'^* \partial z'^*}} = 0, \tag{15}$$

in which

$$\zeta'^* = -\partial(U/U_b)/\partial(y'/D_h) \equiv \zeta' D_h/U_b$$

and ζ' is the vorticity component of the mean flow directed along the z' axis (refer to figure 10). In (15) each term can be interpreted as either a loss or gain in

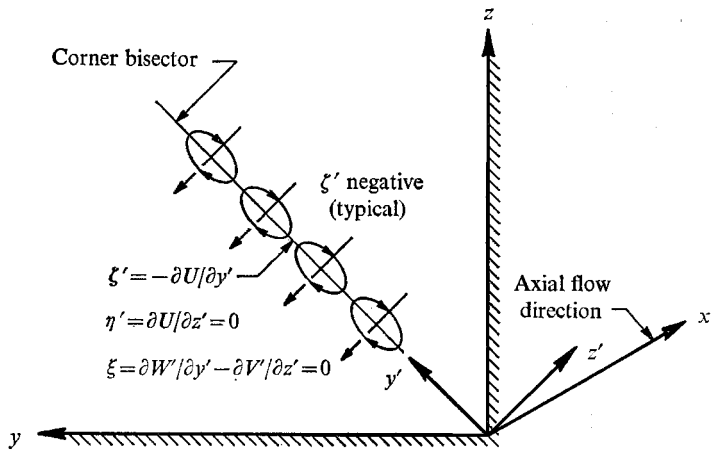

FIGURE 10. Behaviour of the ξ, η' and ζ' components of mean flow vorticity along the corner bisector $z' = 0$ for fully developed flow.

mean flow vorticity within an inertial volume element on the corner bisector depending, respectively, on whether the term is a positive or negative quantity. The terms in (15) represent the convective transport of primary-flow vorticity by the secondary flow (I), the viscous diffusion of primary-flow vorticity (II A and II B) and the change in mean flow vorticity that occurs because of the combined effect of time-averaged convection of turbulent vorticity by the turbulent motion and the time-averaged production of turbulent vorticity by the stretching of turbulent vortex lines (III A and III B).

In accordance with earlier comments it is reasonable to presume that the losses in mean flow vorticity associated with III B in (15) are primarily responsible for the initiation of a transverse convective transport of primary-flow vorticity. This hypothesis was examined by evaluating each term in (15) from the experimental data of the present study. The results are shown in figure 11. In the region near the corner ($0 < y'/a' \lesssim 0{\cdot}3$) the results indicate that a net transport of turbulent vorticity by the turbulent motion into volume elements on the bisector, coupled with the production of turbulent vorticity within these elements (III B), leads to a loss of mean flow vorticity which can only be balanced by a net convective transport of primary-flow vorticity into these elements by the secondary flow (I). The viscous diffusion of primary-flow vorticity (II A and II B) is essentially negligible over most of the boundary layer, and the contribution of turbulent shear stress gradients along the bisector to losses in mean flow vorticity (III A) is also negligible, except in the near vicinity of the corner, where III A is still, however, significantly less than III B. In the outer portion of the boundary layer ($y'/a' \gtrsim 0{\cdot}6$) III A and III B are approximately equal in magnitude, but of opposite sign, and therefore convective transport of primary-flow vorticity by the secondary flow is negligible in this region. On the basis of these and earlier results, it is apparent that vorticity and energy of the mean flow are convected inwards towards a corner as a direct result of transverse turbulent shear stress gradients in the flow.

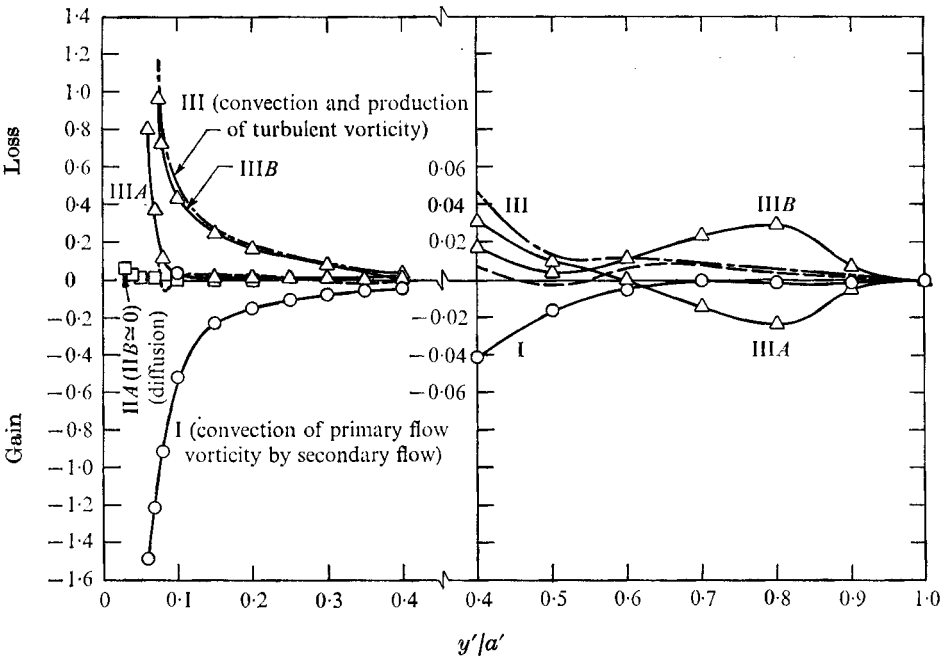

FIGURE 11. Vorticity balance for the mean motion along the corner bisector $z' = 0$; $Re_b = 2{\cdot}5 \times 10^5$. – – –, I+II+III.

The mechanisms which influence secondary flow directed away from the bounding walls of a corner (refer to figure 1) are also of interest and can be analysed to a certain extent by examining the nature of flow along a wall bisector of a square channel when the flow is fully developed. In order to examine the possible influence of transverse turbulent shear stress gradients on the flow, consider the isotach patterns shown in figure 12, which are based on data taken in the present study and are representative of similar data obtained in related studies. From the figure it is apparent that the curvature of isotachs in the vicinity of the wall bisector $z = a$ changes from convex to concave when viewed along the y axis. The behaviour is similar to that which occurs when the flow is developing (cf. the changes in isotach curvature which occur along the line $z/a = 0{\cdot}3$ at $x/D_h = 8$ in figure 4), and consequently the discussion and results which follow should also be applicable at locations where similar changes in isotach curvature occur in a developing flow.

It will first be noted that the foregoing arguments which were used to deduce that $\overline{uw'}$ is positive for $z' > 0$ and negative for $z' < 0$ can also be used to deduce that $\overline{uw}$ values should be positive and negative on either side of $z = a$ as shown in figure 12. The results shown in figure 13 support this contention and are based on data taken at transverse intervals of 0·25 in. ($\Delta z/a = 0{\cdot}05$) along normals to the wall bisector. These results indicate that the transverse shear stress gradient at points along the bisector is first negative for $0{\cdot}05 \leqslant y/a \lesssim 0{\cdot}6$ and then positive for $0{\cdot}6 < y/a \leqslant 1{\cdot}0$. This behaviour is in agreement with the anticipated change in sign of this gradient that should occur along the bisector (refer to figure 12).

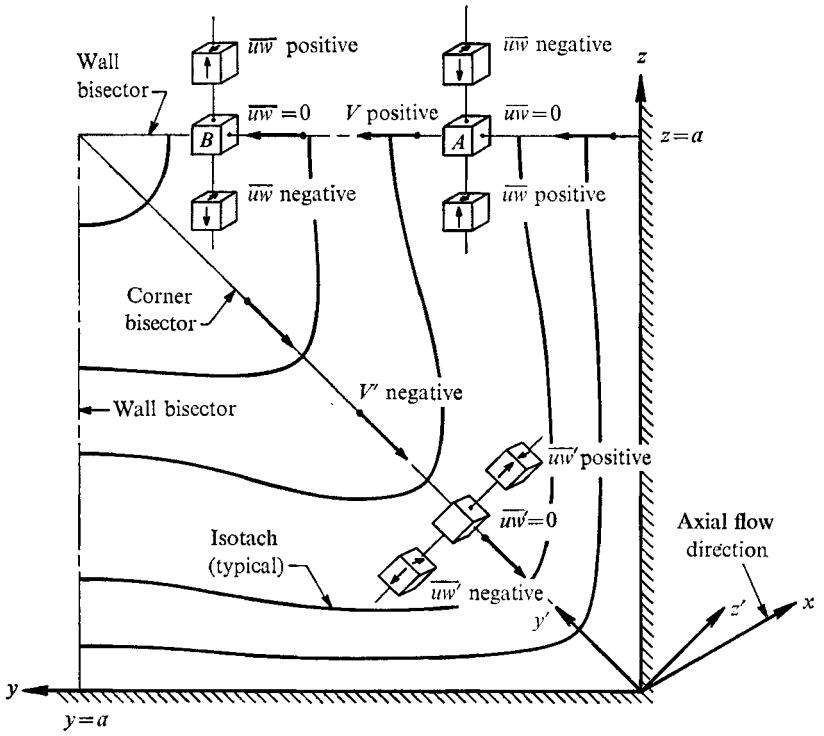

FIGURE 12. Predicted behaviour of $\overline{uw}$ and $\overline{uw'}$ stress components in the vicinity of wall and corner bisectors for fully developed flow.

The results also indicate, however, that non-zero $\overline{uw}$ values were measured on the wall bisector, when, indeed, these values should be zero in accordance with symmetry considerations. This behaviour is attributable to a slight asymmetry of the flow which was observed in the vicinity of the wall bisector. The degree of asymmetry was most pronounced in the near-wall region, e.g. at $y/a = 0{\cdot}05$, but did not lead to difficulties in evaluating the transverse shear stress gradient at this point or at other points along the bisector.

A comparison between the results shown in figure 13 and isotach patterns in the near vicinity of the wall bisector (figure 12) shows that transverse shear stress gradients are not necessarily small in regions where changes in isotach curvature are relatively mild. The influence of these gradients on maintenance of secondary flow directed away from a wall was examined by experimentally evaluating the terms of an energy balance written along the wall bisector $z = a$. The non-dimensionalized energy balance which applies after the boundary-layer approximations have been introduced is as follows:

$$\underset{IA}{U^*\frac{\partial P_0^*}{\partial x^*}}+\underset{IB}{V^*\frac{\partial P_0^*}{\partial y^*}}-\underset{IIA}{\frac{1}{Re_b}\left[\frac{\partial}{\partial y^*}\left(U^*\frac{\partial U^*}{\partial y^*}\right)\right]}+\underset{IIB}{\frac{\partial}{\partial z^*}\left(U^*\frac{\partial U^*}{\partial z^*}\right)}$$

$$+\underset{IIC}{\frac{\partial}{\partial y^*}(U^*\overline{uv}^*)}+\underset{IID}{\frac{\partial}{\partial z^*}(U^*\overline{uw}^*)}-\underset{III}{\overline{uv}^*\frac{\partial U^*}{\partial y^*}}+\underset{IV}{\frac{1}{Re_b}\left(\frac{\partial U^*}{\partial y^*}\right)^2}=0, \quad (16)$$

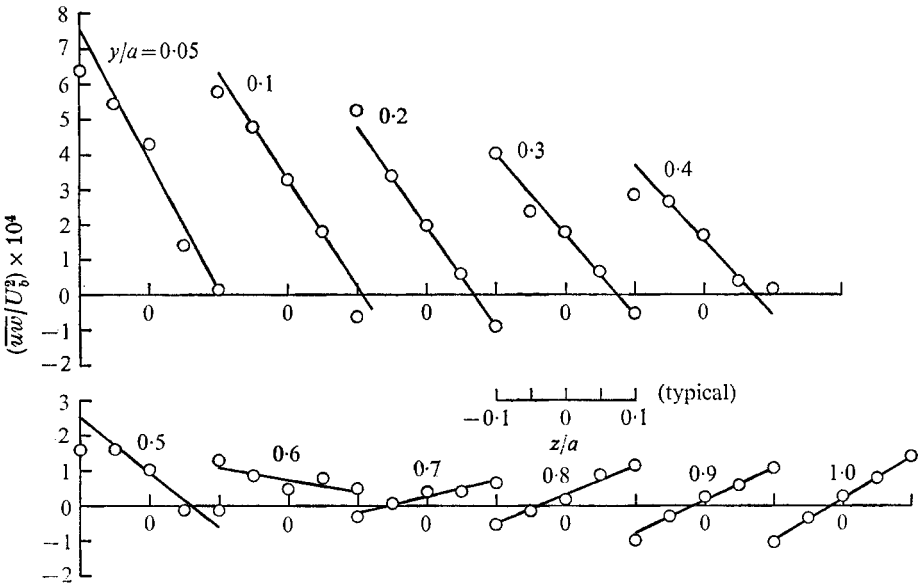

FIGURE 13. Turbulent shear stress distributions along normals to the wall bisector $z = a$; $Re_b = 2{\cdot}5 \times 10^5$.

where all of the variables have been normalized by the same normalizing factors as those introduced earlier and the physical interpretation of each term is the same as that of its counterpart in (14).

In accordance with earlier comments, the term IID in (16) should first be negative in the inner portion of the boundary layer ($0 < y < y_0$) and then positive in the outer portion of this layer ($y_0 < y < a$), where y_0 is defined as that value of y at which $\partial(U^*\overline{uw}^*)/\partial z^* = 0$. Since the convective transport term $V^*\partial P_0^*/\partial y^*$ in (16) is positive for $0 < y < a$, it is apparent that the roles of IB and IID in (16) over the interval $0 < y < y_0$ are now reversed from those of their counterparts in (14). More specifically, it would now appear that the working of the mean flow against transverse shear stress gradients in the inner region causes a net influx of energy into a volume element on the bisector (e.g. element A in figure 12), which necessarily leads to a net efflux of energy from the element through convective transport by the secondary flow. It should be noted, however, that because of the relatively gentle changes in isotach curvature which occur in the near vicinity of the bisector (refer to figure 12), transverse shear stress gradients along the bisector are likely to be an order of magnitude less than their counterparts along a corner bisector. This behaviour, in turn, implies that other factors may also significantly influence the secondary flow. Indeed, in the outer region of the boundary layer there must be one or more mechanisms other than transverse shear stress gradients which maintain the secondary flow because IB and IID in (16) are both positive, i.e. each term is indicative of a net efflux of energy from a volume element, such as element B, on the bisector.

The degree of complexity of the energy fluxes associated with an outwardly directed secondary flow is illustrated in figure 14, where the distributions shown are based on measurements along and normal to the wall bisector $z = a$. In

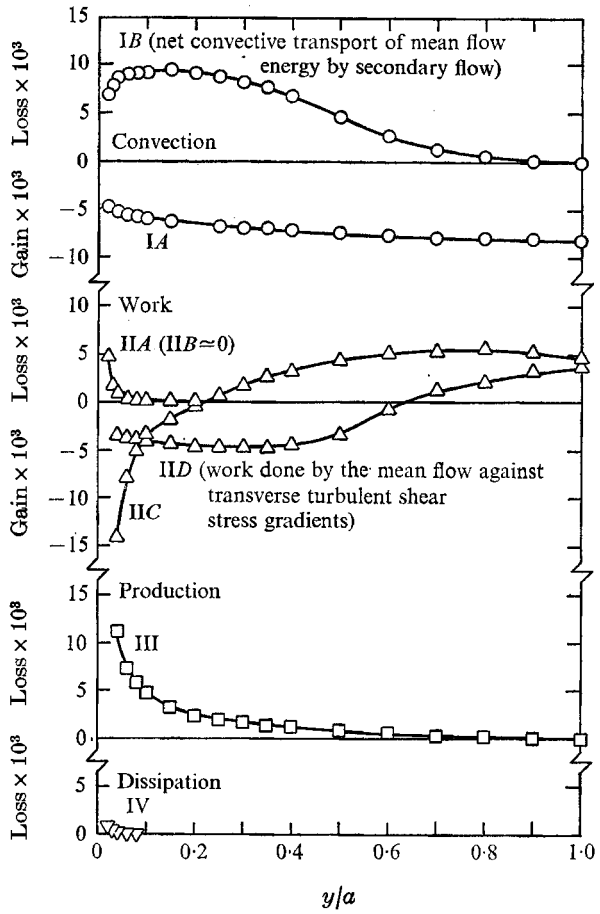

FIGURE 14. Distribution of terms in (16) along the wall bisector $z = a$; $Re_b = 2{\cdot}5 \times 10^5$.

contrast to the results shown in figure 8, all energy terms are now of the same order of magnitude, with the exception of the dissipation term (IV), which is still negligible over most of the boundary layer. As anticipated, the convective transport term associated with the secondary flow (I B) is indicative of a net loss in mean flow energy within volume elements on the bisector, whereas the working of the mean flow against transverse turbulent shear stress gradients in the flow (II D) can yield either a net gain or loss of energy within an element depending on its location from the wall. In the near-wall region ($y/a \simeq 0{\cdot}1$) the energy gained by the working of the mean flow against turbulent shear stress gradients along the bisector (II C) is essentially balanced by the losses incurred by the production of turbulent energy from the mean flow (III). In this region, therefore, convective transport of mean flow energy by the primary (I A) and secondary (I B) flows causes a net efflux of energy which is approximately balanced by the gain in energy which occurs as a result of work done on the mean flow by transverse shear stress gradients in the flow (II D). In the outer region of the boundary layer ($y/a > 0{\cdot}6$), I A is negative, II C and II D are both positive and the net energy flux

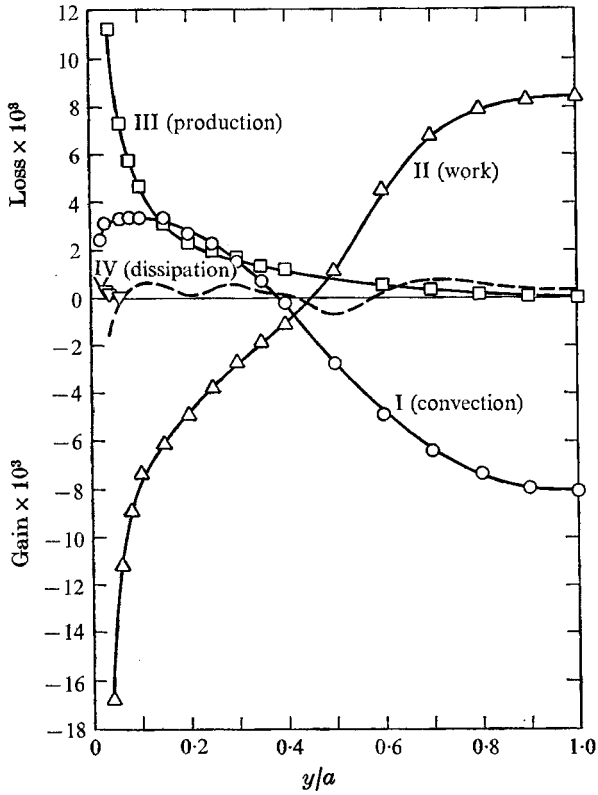

FIGURE 15. Energy balance for the mean motion along the wall bisector $z = a$; $Re_b = 2{\cdot}5 \times 10^5$. – – – –, I+II+III+IV.

associated with the sum of these terms serves to maintain a weak secondary flow in this region.

The distributions shown in figure 14 are plotted in alternative form in figure 15, where the sum of terms is indicative of the overall accuracy of the measurements. On the basis of these and earlier results, it is apparent that the interactions which occur between the mean flow and its associated turbulence structure are relatively complex for turbulent flow along a corner. The complexity of these interactions does not, however, lead to difficulties in interpreting the results or in identifying the origin of secondary flow from either an energy or vorticity point of view.

4. Concluding remarks

The results of the present study show that transverse gradients of Reynolds shear stress components which influence the streamwise shear characteristics of the primary flow, namely $\overline{uv}$ and $\overline{uw}$ or, alternatively, $\overline{uv'}$ and $\overline{uw'}$,† are directly responsible for the generation of secondary flow in turbulent flow along a corner.

† The $\overline{uv'}$ and $\overline{uw'}$ stress components referred to the x, y', z' co-ordinate system (figure 6) are uniquely related to the $\overline{uv}$ and $\overline{uw}$ stress components through the following transformations:

$$\overline{uv'} = \overline{uv}\cos yy' + \overline{uw}\cos zy', \quad \overline{uw'} = \overline{uv}\cos yz' + \overline{uw}\cos zz'.$$

This secondary flow acts as a convective transport mechanism in planes normal to the primary-flow direction. In terms of first-order effects, secondary flow convects momentum (ρU) and vorticity (η and ζ) of the primary flow, as well as the total energy of the mean motion (P_0/ρ). This conclusion follows directly from the momentum, vorticity and energy balances given by (1), (10), (11), (14) and (16), all of which contain terms involving transverse gradients of the $\overline{uv}$ and $\overline{uw}$ stress components.

With reference to second-order effects, it will first be noted that ξ, the streamwise vorticity component of the mean motion, is typically two orders of magnitude less than either η or ζ in a corner region. Previous studies have shown that convective transport of streamwise vorticity by secondary flow is due primarily to the production of turbulent vorticity from the mean flow via transverse gradients of Reynolds stress components which act wholly in planes normal to the primary flow direction, i.e. $\overline{v^2}$, $\overline{w^2}$ and $\overline{vw}$ (cf. equation (12) and results presented by Brundrett & Baines 1964 and Perkins 1970). This conclusion does not contradict the foregoing results, but simply means that other manifestations of the turbulent field are required in order to describe second-order effects.

Similar reasoning applies to the mechanisms responsible for the convective transport of turbulence kinetic energy, k, noting that k is typically two orders of magnitude less than its mean flow counterpart, P_0/ρ. On the basis of results presented by Hinze (1967), it is known that convective transport of turbulence kinetic energy by secondary flow is governed primarily by the production of turbulent energy (via terms of the form $\overline{uv}\,\partial U/\partial y$ and $\overline{uw}\,\partial U/\partial z$) and the dissipation of turbulent energy (via terms involving correlations between components of the instantaneous turbulent rate of strain tensor). Again, however, convective transport of turbulence kinetic energy by secondary flow is a second-order effect, and one would anticipate that mechanisms other than those associated with transverse gradients of the $\overline{uv}$ and $\overline{uw}$ stress components would govern the overall process.

The implications of the foregoing results on the generation of secondary flow in other flow situations merit further comment. In general, it would appear that whenever variations in isotach curvature occur in a laminar flow undergoing transition, transverse turbulent shear stress gradients are generated along an isotach which necessarily give rise to a transverse flow directed from the concave toward the convex side of the isotach. If this statement is valid, it would explain the appearance of secondary flows which have been observed in other flow situations, such as turbulent flow over an external corner (Nikuradse 1930) and turbulent flow over a flat plate of finite width (Elder 1960). The consistency of this argument with the physical flow situation for each case can be illustrated by considering an approximate form of (13), namely

$$\underset{\text{I}B}{\frac{V'}{\rho}\frac{\partial P_0}{\partial y'}} + \underset{\text{II}D}{\frac{\partial}{\partial z'}(U\overline{uw'})} \simeq 0, \tag{17}$$

which should be roughly applicable in an edge or corner region, where the energy transfer mechanisms associated with terms IB and IID are likely to dominate

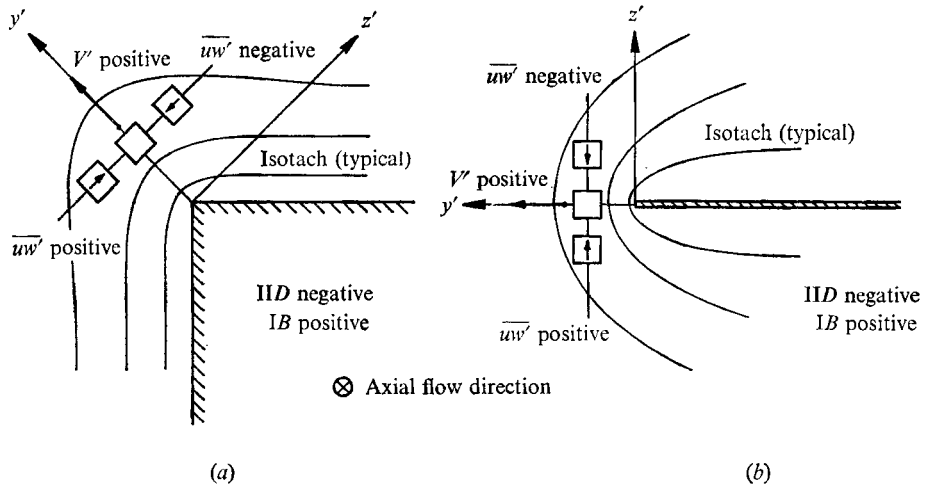

FIGURE 16. Predicted behaviour of $\overline{uw'}$ stress component and V' component of secondary flow in other flow situations. (*a*) External corner flow. (*b*) Flow over a flat plate of finite width.

the flow. The anticipated sign of IID in the region where changes in isotach curvature are maximal for each case is shown in figure 16 for early transitional flow. In accordance with earlier comments it is reasonable to presume that IID will be negative in the transition region, even though the flow is only intermittently turbulent. This behaviour, in turn, implies that IB will be positive, and consequently a transverse flow will be generated which is directed as shown on each diagram. It may be noted that the indicated outward direction of the secondary flow for each case is consistent with the experimental observations of Nikuradse (1930) and Elder (1960). Similar arguments can be applied to deduce the direction of secondary flow in a bounded rectangular turbulent jet and in turbulent flow over a flat plate with a transverse variation in wall roughness, as observed by Foss & Jones (1968) and Hinze (1967), respectively. In both types of flow, variations in isotach curvature exist when the flow is laminar which may well lead to the development of secondary flow via the mechanism described in the present paper when the flow becomes turbulent. The applicability of the foregoing arguments to these and other related flow situations should be the subject of further study.

This study was made possible by a grant from the National Science Foundation (NSF GK 2130). The author would like to express his gratitude to the Foundation for their support of this work. The author would also like to thank Mr Richard J. Page and Dr Ross A. Fiedler for their assistance with some of the initial measurements.

Appendix. Experimental apparatus and measurement techniques

The measurements were made in a square channel lined with Formica and joined to a smoothly contoured contraction made of molded fibreglass. The contraction was preceded by an inlet section composed of a plenum chamber with screens, a honeycomb, and a filter section. The width of the channel between opposite interior walls was maintained at $10 \pm 0{\cdot}010$ in. and the bounding walls of each corner were perpendicular to within $\pm 0{\cdot}05°$. Air was drawn into the inlet section by means of a centrifugal fan located downstream of the channel exit and the flow was allowed to develop in the absence of a tripping device at the channel inlet. All probes were positioned by means of a traversing mechanism with a movable plate whose inner surface was maintained flush with the interior surface of one channel wall. Static pressure taps mounted on the movable plate were used to monitor the local wall static pressure. A miniature Kiel probe was used in conjunction with one of these taps to measure boundary-layer profiles and isotach patterns in the channel. Secondary-flow velocity components were measured by means of a single-wire rotation technique developed by Hoagland (1960) and subsequently modified by Gessner (1964).

Turbulent shear stress measurements were made with a 0·00015 in. diameter tungsten wire having an active length of $\sim 0{\cdot}030$ in. which was inclined at a nominal angle of 45° with respect to the axial flow direction. The wire was mounted on a probe aligned with the axial flow direction and rotation of the probe about its centre-line axis permitted the wire to be positioned in two different positions in each plane of interest, i.e. in the xy, xy', xz or xz' plane. The wire was operated at constant temperature by means of a Thermo-systems Model 1010 anemometer and was calibrated periodically in fully developed turbulent pipe flow.

In order to correlate velocity fluctuations with voltage fluctuations across the wire, the following energy balance was assumed to apply instantaneously to the wire:

$$E^2 = A + BU_e^n, \tag{18}$$

where E is the instantaneous voltage across the wire, A and B are temperature-dependent coefficients which were assumed to be constant, U_e is the instantaneous effective cooling velocity, and n is an exponent whose value depends, in general, on the local flow conditions. If the wire is assumed to lie in the x, y plane, then, on the basis of results presented by Hill & Sleicher (1969), U_e can be represented as

$$U_e = (U+u)\cos\alpha(1+k^2\tan^2\alpha)^{\frac{1}{2}} + v\sin\alpha(1-k^2)/(1+k^2\tan^2\alpha)^{\frac{1}{2}}, \tag{19}$$

where α is the angle between the normal to the wire and the axial flow direction and k is a factor which accounts for tangential cooling effects along the wire. An expression for $\overline{uv}/U^2$ in terms of bridge output voltages from the anemometer can be developed by substituting the expression for U_e into (18) and time averaging the results. The resulting expression is

$$-\frac{\overline{uv}}{U^2} = K(\alpha, k, n)\left[\frac{\bar{E}_b^2\,|\overline{e_{b1}^2} - \overline{e_{b2}^2}|}{(\bar{E}_b^2 - \bar{E}_{b0}^2)^2}\right], \tag{20}$$

in which $K(\alpha, k, n) = (1 + k^2 \tan^2 \alpha)/[n^2(1 - k^2) \tan \alpha]$, $\bar{E}_b$ and $\bar{E}_{b0}$ are mean bridge output voltages for heated and unheated conditions, respectively, and $\overline{e_{b1}^2}$ and $\overline{e_{b2}^2}$ are mean-square voltages of the bridge voltage fluctuations with the wire in positions 1 and 2 (i.e. inclined at $\pm \alpha$) in the x, y plane.

Instead of attempting to estimate $K(\alpha, k, n)$ from explicit values of α, k and n, this factor was evaluated by means of an iterative procedure as follows. The inclined wire probe was initially located in fully developed turbulent pipe flow, where it was assumed that

$$-\frac{\overline{uv}}{\overline{U^2}} = \frac{u_\tau^2}{\overline{U^2}}\left(1 - \frac{y}{R}\right), \quad 0{\cdot}1 \leqslant y/R \leqslant 1{\cdot}0, \tag{21}$$

in which R is the pipe radius, y is the perpendicular distance from the wall, and u_τ is the friction velocity, as evaluated from static pressure drop measurements along the pipe. The wire was traversed across the pipe radius and values of $\overline{uv}/\overline{U^2}$ were evaluated from (20) for an estimated nominal value of K under flow conditions similar to those in the channel. These values were compared with their counterparts predicted from (21) and K was then adjusted to give the best least-squares fit of the data to the analytical distribution. By following this procedure, it was possible to determine $K(\alpha, k, n)$ directly without having to measure the angle of inclination α, or determine a value for k (e.g., from the results of Champagne, Sleicher & Wehrmann 1967), or even estimate an appropriate value for n. This approach facilitated the reduction of turbulence data and led to consistent and repeatable results.

REFERENCES

Brundrett, E. 1963 The production and diffusion of vorticity in channel flow. *Dept. Mech. Engng, University of Toronto, Rep.* TP 6032.

Brundett, E. & Baines, W. D. 1964 The production and diffusion of vorticity in duct flow. *J. Fluid Mech.* **19**, 375–394.

Champagne, F. H., Sleicher, C. A. & Wehrmann, O. H. 1967 Turbulence measurements with inclined hot wires. Part 1. Heat transfer experiments with inclined hot-wire. *J. Fluid Mech.* **28**, 153–175.

Eichelbrenner, E. A. & Preston, J. H. 1971 On the role of secondary flow in turbulent boundary layers in corners (and salients). *J. Mécanique*, **10**, 91–112.

Eichelbrenner, E. A. & Toan, N. K. 1969 A propos des vitesses secondaires dans la couche limite turbulente à l'intérieur d'un dièdre. *Comptes Rendus*, **269**, 869–872.

Einstein, H. A. & Li, H. 1958 Secondary currents in straight channels. *Am. Geophys. Un.* **39**, 1085–1088.

Elder, J. W. 1960 The flow past a flat plate of finite width. *J. Fluid Mech.* **5**, 133–153.

Foss, J. & Jones, J. B. 1968 Secondary flow effects in a bounded rectangular jet. *J. Basic Engng, Trans. A.S.M.E.* **90**, 241–248.

Gessner, F. B. 1964 Turbulence and mean-flow characteristics of fully developed flow in rectangular channels. Ph.D. thesis, Purdue University.

Gessner, F. B. & Jones, J. B. 1961 A preliminary study of turbulence characteristics of flow along a corner. *J. Basic Engng, Trans. A.S.M.E.* **83**, 657–662.

Gessner, F. B. & Jones, J. B. 1965 On some aspects of fully developed turbulent flow in rectangular channels. *J. Fluid Mech.* **23**, 689–713.

Hill, J. C. & Sleicher, C. A. 1969 Equations for errors in turbulent measurements with inclined hot wires. *Phys. Fluids*, **12**, 1126–1127.

HINZE, J. O. 1959 *Turbulence*. McGraw-Hill.

HINZE, J. O. 1967 Secondary currents in wall turbulence. *Phys. Fluids*, **10** (suppl.), S 122–S125.

HOAGLAND, L. L. 1960 Fully developed turbulent flow in straight rectangular ducts – secondary flow, its cause and effect on the primary flow. Ph.D. thesis, Department of Mechanical Engineering, Massachusetts Institute of Technology.

NIKURADSE, J. 1926 Untersuchungen über die Geschwindigkeitsverteilung in turbulenten Strömungen. Thesis, Göttingen. (See also *Forschungsh. Ver. dtsch. Ing.*, **281**.)

NIKURADSE, J. 1930 Turbulente Strömung in nicht kreisförmigen Rohren. *Ing. Arch.* **1**, 306–332.

PERKINS, H. J. 1970 The formation of streamwise vorticity in turbulent flow. *J. Fluid Mech.* **44**, 721–740.

PRANDTL, L. 1926 Über die ausgebildete Turbulenz. *Verh. 2nd Int. Kong. für Tech. Mech. Zürich*, pp. 62–75. (Trans. *N.A.C.A. Tech. Memo.* no. 435.)

PRANDTL, L. 1952 *Essentials of Fluid Dynamics*. London: Blackie.

TOWNSEND, A. A. 1961 Turbulence. In *Handbook of Fluid Dynamics* (ed. V. L. Streeter), §§ 10.1–10.33. McGraw-Hill.

ZAMIR, M. & YOUNG, A. D. 1970 Experimental investigation of the boundary layer in a streamwise corner. *Aero. Quart.* **21**, 313–339.